NFCStack: Identifiable Physical Building Blocks that Support Concurrent Construction and Frictionless Interaction

Chi-Jung Lee
National Taiwan University
Taipei, Taiwan
cjlisalee@cmlab.csie.ntu.edu.tw

Rong-Hao Liang
Eindhoven University of Technology
Eindhoven, The Netherlands
r.liang@tue.nl

Ling-Chien Yang
National Taiwan University
Taipei, Taiwan
natalieyang@cmlab.csie.ntu.edu.tw

Chi-Huan Chiang
National Taiwan University
Taipei, Taiwan
chihuan@cmlab.csie.ntu.edu.tw

Te-Yen Wu
Dartmouth College
Hanover, USA
te-yen.wu.gr@dartmouth.edu

Bing-Yu Chen
National Taiwan University
Taipei, Taiwan
robin@ntu.edu.tw

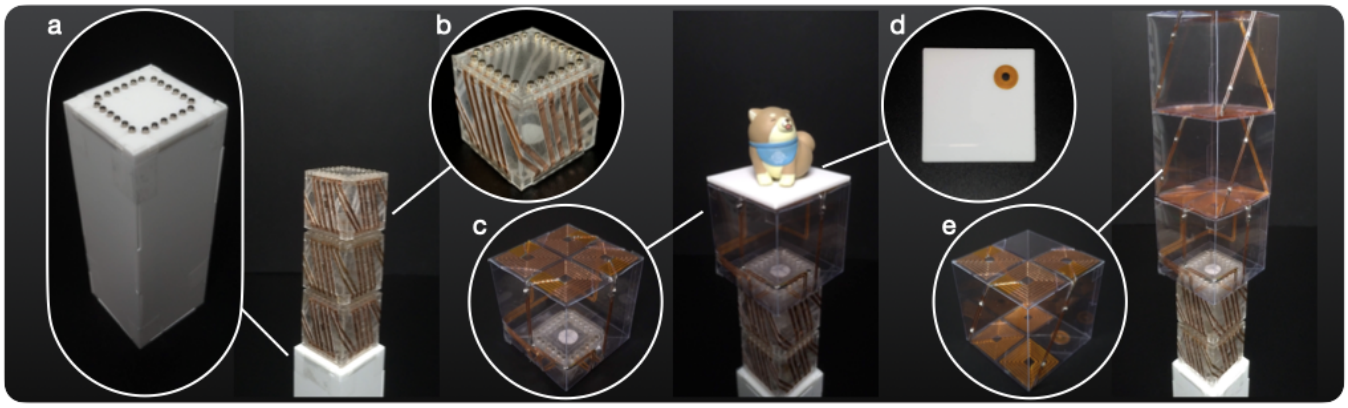

Figure 1: NFCStack is a physical building block system that supports rich-ID stacking and interaction. The system consists of (a) portable *stations*, into each of which a multiplexed near-field communication (NFC) reader is embedded; (b) identifiable *bricks* that enable sturdy construction; and (c) identifiable *adapters* that convert the top of a stack into a few portals of the NFC reader, so that they can detect and identify (d) an NFC-tagged token's orientation and (e) events in which the identifiable *boxes* are stacked.

ABSTRACT

In this paper, we propose NFCStack, which is a physical building block system that supports stacking and frictionless interaction and is based on near-field communication (NFC). This system consists of a portable station that can support and resolve the order of three types of passive identifiable stackable: bricks, boxes, and adapters. The bricks support stable and sturdy physical construction, whereas the boxes support frictionless tangible interactions. The adapters provide an interface between the aforementioned two types of stackable and convert the top of a stack into a terminal for detecting interactions between NFC-tagged objects. In contrast to existing systems based on NFC or radio-frequency identification technologies, NFCStack is portable, supports simultaneous interactions, and resolves stacking and interaction events responsively, even when objects are not strictly aligned. Evaluation results indicate that the proposed system effectively supports 12 layers of rich-ID stacking with the three types of building block, even if every box is stacked with a 6-mm offset. The results also indicate possible generalized applications of the proposed system, including 2.5-dimensional construction. The interaction styles are described using several educational application examples, and the design implications of this research are explained.

CCS CONCEPTS

• **Human-centered computing** → **User interface toolkits**; **Ubiquitous and mobile computing systems and tools**; **Interaction design theory, concepts and paradigms**.

KEYWORDS

NFC, building blocks, stacking, tangible interaction

ACM Reference Format:
Chi-Jung Lee, Rong-Hao Liang, Ling-Chien Yang, Chi-Huan Chiang, Te-Yen Wu, and Bing-Yu Chen. 2022. NFCStack: Identifiable Physical Building

UIST '22, October 29-November 2, 2022, Bend, OR, USA

ACM ISBN 978-1-4503-9320-1/22/10.
https://doi.org/10.1145/3526113.3545658

Blocks that Support Concurrent Construction and Frictionless Interaction. In *The 35th Annual ACM Symposium on User Interface Software and Technology (UIST '22), October 29-November 2, 2022, Bend, OR, USA.* ACM, New York, NY, USA, 12 pages. https://doi.org/10.1145/3526113.3545658

1 INTRODUCTION

Stacking is a common task in the process of spatio temporal organization, such as the grouping or ordering of items. [30]. Compared with two-dimensional (2D) clustering, stacking is a space-saving method for extending the property of an object while stabilizing its location. Therefore, human-computer interaction (HCI) researchers are seeking technological solutions for harnessing stacks as a form of tangible interface [18] to leverage our existing cognitive and spatial knowledge to comprehend the embodied digital information.

Passive radio-frequency identification (RFID) and near-field communication (NFC) technologies have been adopted by HCI researchers because these technologies have a virtually infinite ID space, are relatively unaffected by the line-of-sight problem, and involve straightforward maintenance. Although RFID does not support the resolution of tagged object stacking, researchers have proposed the use of contact switches [17] or a collision avoidance mechanism [41] to resolve the order of stacking of RFID-tagged objects from sequential stack events. However, difficulties occur when using the aforementioned technologies to simultaneously resolve concurrent stack events originating from multiple input sources.

In this paper, we propose NFCStack (Figure 1), which is a physical building block system that supports stacking and interaction based on NFC. The extendable antenna design used in this system enables a multiplexed NFC reader to track the stack event at every height through a different channel so that concurrent actions can be resolved. Moreover, robust and responsive stack tracking can be achieved with this design.

To ensure that the system can support both rich-ID stacking and tangible interaction, the proposed system comprises three types of passive identifiable stackable object: brick, box, and adapter. The bricks are connected through magnetic connectors, which result in a sturdy and stable physical construction. By contrast, the boxes support frictionless tangible interaction because they are wirelessly connected using conductor coils. The adapter provides an interface between the bricks and the boxes and converts the top of a stack into multiple terminals for detecting interaction events on the top of the stack, such as an NFC-tagged token's orientation or stack events of the identifiable boxes.

We implemented the proposed system to test its performance. The evaluation results indicate that the proposed system effectively supports 12 layers of rich-ID stacking with the three types of building block, even if every box is stacked with a 6-mm offset. The results also indicate possible generalized applications of the proposed system, including 2.5-dimensional (2.5D) construction. This paper describes the interaction styles supported by the proposed system by using several application examples.

The main contribution of this work is the design, engineering, and development of a physical building block system that can resolve concurrent stacking and combine the stable construction and frictionless input modes into conventional NFC interaction.

The rest of this paper is organized as follows. Section 2 presents a description of related work. Section 3 describes the design, implementation, and evaluation of the proposed system. Finally, Section 4 details the design implications of this work and provides directions for future research.

2 RELATED WORK

2.1 Constructive Assembly and Stackables

Constructive assemblies of modular interconnecting elements facilitate physical modeling and the production of geometrical representations, such as Lego bricks [1] and Meccano [2]. The application of constructive assemblies in HCI as tangible user interfaces [18, 40] can facilitate reality-based interactions that leverage users' body, social, and environmental awareness and skills as well as their common knowledge regarding Euclidean physics [19]. Rich embodied and kinetic experiences can be useful in various tasks, especially in the learning of abstract concepts [44] or exploration of design opportunities [14, 35, 37].

Stacking enables the construction of three-dimensional (3D) building blocks. Researchers have used embedded electronic circuits and sensors, such as motion sensors [16], infrared sensor arrays [4], and conductive dot patterns [12], to detect stack events. However, at scale, these power electronic devices have high deployment and maintenance costs. Researchers have also used passive sensing solutions — such as optical markers [7], marked fiber-optic bundles [8], capacitive footprints [9], pressure images [22], magnetic-field images [24, 27], and radar [43] — to detect the state of stacking through use of an external sensor. However, the ID space and stacking height are limited when using these solutions.

2.2 Identifiable building blocks

Identifiable building blocks can support the semantic construction of information. Scholars have constructed identifiable building blocks into which microcontrollers and/or power-line communication protocols (e.g., I^2C) have been embedded to identify the building blocks used for semantic construction in built geometry [3, 13, 20, 21, 33, 36]. These blocks facilitate high interactivity between the sensors and actuators to which they are connected. However, reducing the electromechanical interconnections of the aforementioned building blocks is not always a straightforward task; thus, these blocks usually support only fixed, rigid constructions and cannot reliably detect objects that are not strictly aligned. Moreover, the blocks have significant hardware and maintenance when they are deployed at scale.

Passive RFID technologies involve straightforward maintenance when they are deployed at scale, so they were used in rapid prototyping human-computer interfaces [23]. RFIBricks [17] is a rich-ID building block system based on modified ultra-high-frequency (UHF) RFID tags. The design harnesses the near-field effects of a far-field UHF RFID system by allowing a unique pair of normally off tags to be turned on simultaneously during stacking. Consequently, the aforementioned system involves a volumetric interaction stage in which the building block units remain passive. The RFIBricks system requires strict alignment between building blocks, and this

[1] http://www.lego.com/
[2] www.meccano.com

alignment is achieved using magnetic connectors that require more effort for the users to perform stacking and unstacking operations. Although a follow-up work RFIMatch [26] indicated that a correlated state change can be achieved without the need for physical contact between objects by incorporating a magnet-biased reed switch mechanism. How such a mechanism can be implemented in a building block system is unknown.

The most fundamental limitation of the UHF RFID approach is that the interaction area is defined by the antenna connected to the bulky, high-power-consumption, and expensive UHF reader. Additionally, the building blocks cannot be effectively miniaturized because of tag-to-tag interference when tags are deployed at high-density. Finally, the aforementioned approach does not support concurrent events, which frequently occur in multi-user or bimanual interactions with small objects.

Previous work has explored the design spaces of passive rich-ID building blocks with NFC. Project Zanzibar [41] explored rich-ID stacking with NFC by using a relay coil structure, namely Stacker, to extend power and data transfer from the mat of the NFC antenna matrix to the upper layers of the stack. When a user sequentially stacks one layer on the other, new tags can be activated and read using the Dynamic Frame Slotted ALOHA (DFSA) [10] collision avoidance mechanism. Similar to RFIBricks, the Zanzibar system does not support concurrent events because the order of simultaneous multitag appearances cannot be guaranteed in NFC. Furthermore, the response time of the Zanzibar system linearly increases with the layer number of the stack because of the nature of the DFSA algorithm, and this results in lower reliability and poorer user experience at higher levels of the stack. The delays make common stack operations (e.g., re-ordering) inefficient and unreliable.

2.3 Tangible Interaction with NFC

NFC and high-frequency RFID (HF RFID) systems have been broadly used in tangible interactions for identifying passive tagged objects [6, 31, 38]. Compared with sensing technologies based on electromagnetic induction, such as those developed in [34, 39], NFC and RFID systems, which are off-the-shelf technologies, can be used more easily for prototyping. The near-field sensing range of NFC and RFID systems enables contactless and therefore frictionless interaction. In addition to popular toy-to-life applications, such as Nintendo Amiibo [3] and Lego Dimensions [4], researchers have used off-the-shelf NFC tags for sensing user inputs, such as speed and frequency [25], and have employed multiple tags in compound widgets (e.g., sliders, knobs) for tangible interaction [5, 15, 25]. In this paper, we aimed to achieve concurrent construction and frictionless tangible interaction with the NFCStack system.

3 ANTENNA EXTENSION METHODS

To identify an NFC-tagged block placed on top of a stack of blocks on a station, the blocks shall extend the detection range of the underlying reader's antenna to the top surface. Section 3.1 explains the theoretical background of this work, and Section 3.2 describes the two antenna coil extension methods used in this paper: transmission line extension and multihop extension.

[3]https://www.nintendo.com/amiibo
[4]https://www.lego.com/en-us/dimensions/products

3.1 Background

NFC readers and tags operate at $f = 13.56MHz$. To construct wireless antennas that harness the power and signals of NFC readers and tags, an RLC resonant circuit is required, where R, L, and C represent a resistor, an inductor, and a capacitor, respectively.

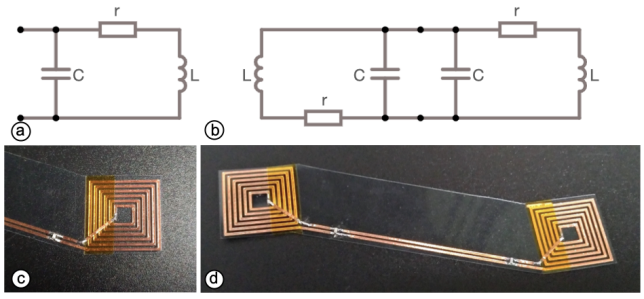

Figure 2: Schematics of a (a) half relay and a (b) full relay as well as photographs of the (c) half relay and (d) full relay fabricated in this paper.

Figure 2a displays the schematic of a typical RLC circuit, which is termed a *half relay* in this paper. A suitable R, L, and C must be selected such that two conditions are satisfied: 1) $f_0 = \frac{1}{2\pi}\sqrt{\frac{1}{LC} - (\frac{R}{L})^2} \sim f$, where f_0 is the resonant frequency of the RLC circuit, and 2) $Q = \frac{1}{R}\sqrt{\frac{L}{C}}, 30 \geq Q > 1$ where Q is the quality factor of the RLC circuit. A Q value of 30 is the theoretical upper bound for ensuring sufficient bandwidth for full-speed (424-kbit) NFC. When the aforementioned two conditions are satisfied, an RLC circuit can effectively and efficiently resonate at the frequency $f_0 \sim f$.

Figure 2a displays a schematic of a full relay, which can be used for extending the NFC reader antenna's read range [11, 28, 42]. A full relay consists of two half relays connected by transmission lines (a pair of parallel conducting wires). One conductor coil receives the NFC signal through magnetic induction and then relays the signal through the transmission lines to the other conductor coil. When two conductor coils from different relays are sufficiently coupled in proximity to each other, power and signals can be wirelessly transferred from one coil to the other.

However, when one conductor coil is coupled with another one over a larger distance, the geometric dimensions of the two conductor coils affect their power transfer efficiency. For instance, if two conductor loop coils L_a and L_b have radii of r_a and r_b, respectively, the coupling coefficient k is expressed as follows:

$$k(x) = \frac{r_a^2 \cdot r_b^2}{\sqrt{r_a \cdot r_b} \cdot [\sqrt{x^2 + max(r_a, r_b)^2}]^3} \quad (1)$$

where x is the lateral distance between L_a and L_b. A k value of 1 can be achieved when $x = 0$ and $r_a = r_b$. However, in practice, inductively coupled transponder systems operate under coupling coefficients that might be as low as $k = 0.01$ ($< 1\%$) [10]. Nevertheless, to enable coils to withstand an offset of x', the use of sufficiently large coils (e.g., $r_a \sim r_b >> x'$) of similar size is preferred.

3.2 Transmission Line Extension

The conductor coil's location can be mechanically extended from the reader by using a pair of parallel transmission lines, as shown in Figure 3a. By adopting low-resistance electromechanical connectors, multiple segments of transmission lines can be connected to extend the transmission line. A physical part with an NFC-tagged coil, which contains two terminals that can be connected to transmission lines, can be identified by an NFC reader when the lines are connected.

The simple method has only a small footprint, which makes it a suitable method for constructing small building blocks. However, this method also requires a firm low-ohmic electromechanical connection,which may impede the HCI because considerable physical effort must be expended to break a strong connection between two blocks. Relaxing the alignment constraint between two blocks without compromising the low-ohmic connection is challenging, if not impossible. Finally, the additional capacitance generated because of an increase in the length of transmission lines may affect the tuning of the RLC circuits.

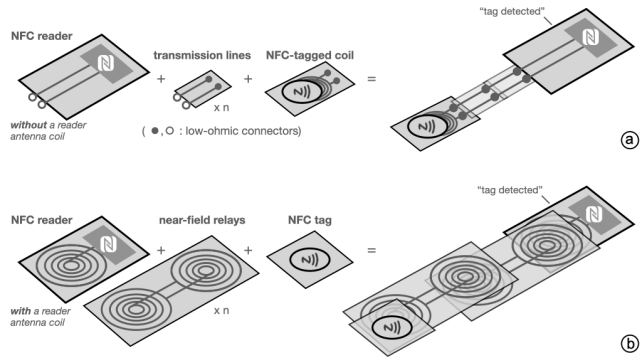

Figure 3: Two antenna extension methods considered in this paper: (a) transmission line extension; (b) multihop extension.

3.3 Multihop Extension

To enable *effortless* interactions, the conductor coils' location can be extended using multiple hops of relay connections, as illustrated in Figure 3b. Therefore, a multi-hop connection with multiple relays segments can be realized without the use of any electromechanical connectors and without physical contact between relays. The coil located at the end of the chained relays serves as an NFC reader that can detect an NFC tag in its near-field region.

Figures 2c and d illustrate a half relay and full relay, respectively, with 2cm-wide rectangular conductor coils that support multihop extension. When using the multihop extension method, conductor coils can effectively transmit power to each other with a sub-centimeter offset; however, this method has a larger footprint than does transmission line extension. When transmission lines are short, the additional capacitance is negligible, and does not affect the tuning of the RLC antenna.

3.4 Summary

Transmission line extension and multihop extension enable a conductor coil to be extended from NFC readers to other locations. These methods have unique advantages, depending on the purpose of use. When the main purpose is to construct a stable physical form, the transmission line extension method provides more rigidity in the construction and enable smaller physical units to be constructed than does the multihop extension method. However, when the main purpose is to achieve tangible interaction, the multihop extension method supports a more versatile set of frictionless tangible interactions than does the transmission line extension method. Therefore, blocks comprising transmission lines are suitable for achieving sturdy construction, whereas blocks comprising near-field relays are suitable for constructing interactive system elements.

Constructive assembly tangible user interface (UI) systems contain constructive and interactive elements. Therefore, a system that is compatible with the aforementioned two types of building block is desirable. A proof of concept forsuch a system is described in Section 4.

4 SYSTEM DESIGN AND IMPLEMENTATION

On the basis of the multihop extension and transmission line extension methods, we designed three types of building block and one *station* that can resolve the stacking order of these blocks. The system design considerations and implementation of the designed system are detailed in the following.

4.1 System Design Considerations

We formulated our design objectives as five design considerations on the form, material, electrical components, connection, and customization of the proposed building block system.

- *Form (D_{form})*: The size of the building blocks should be suitable for one-handed manipulation, and blocks should be cubes or cuboids that support modular stacking and tiling.
- *Material (D_{mtrl})*: The mechanical structure of the building blocks should be sufficiently sturdy to support stacking operations. The conductors deployed on the blocks should be efficiently reduce signal loss in wired and wireless communication.
- *Electrical Component (D_{elec})*: Passive electrical components are employed to reduce maintenance costs. The electrical components in the blocks should be carefully selected and arranged so that they do not impede stacking operations.
- *Connection (D_{conn})*: The connectors between blocks should enable users to perform construction and achieve tangible interaction rapidly and easily. The electrical connection should be reliable so that the system can detect the construction and tangible interaction operations.
- *Customization (D_{cust})*: End users and designers should be able to customize the appearance of the building blocks for creative applications.

4.2 Station

To support concurrent stack events and highly robust and extensible stack sensing, each layer of the stacking must be detected

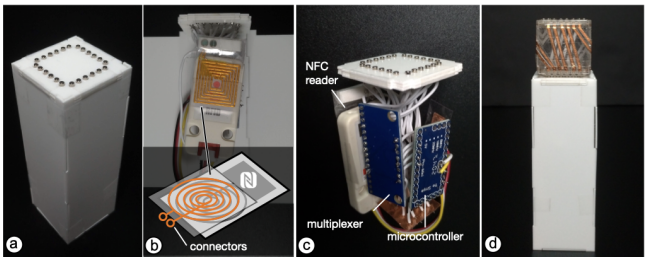

Figure 4: Station: (a) overview, (b) extension of the half relay from the NFC reader antenna, (c) signal processing unit, and (d) a brick on the station.

individually. Therefore, the station contains a multiplexed NFC reader so that high resolution is achieved.

Figure 4 illustrates the station design and an example of its implementation. Each station's top surface is the same as the block's top surface; thus, each station contains M pairs of magnetic connectors ($T^i_{top} = \{T^i_{in}, T^i_{out}\}$, where $1 \le i \le M$) as its terminals on its top surface. T^i_{in} is the input connector of terminal T^i_{top}, and T^i_{out} is the output connector of terminal T^i_{top}. To enable detection of all the NFC tags of multiple blocks stacked on a station, the station contains an NFC reader connected to multiplexer circuitry through the reader's two antenna terminals, namely A_{in} and A_{out}, which are connected to an external half relay. Terminal A_{in} is connected to the input of a 1-to-X multiplexer, whose M (out of the X) output channels are connected to T^i_{in}, and T^i_{out} is connected to A_{out}.

4.3 Building Blocks

The three types of building blocks are *brick*, *box*, and *adaptor*.

4.3.1 Brick. A brick (Figure 5) is an identifiable stackable unit based on the transmission line method. In the case of D_{conn}, each brick has M pairs of magnetic connectors as terminals (T) on its top (T^i_{top}) and bottom (T^i_{bottom}) surfaces, where $1 \le i \le M$. A total of $M-1$ pairs of transmission lines (t_j) are connected between (T^j_{top}) and (T^{j+1}_{bottom}), where $1 \le j \le M-1$. Terminal T^1_{bottom} is connected to a coil at the center of a brick's bottom surface through a pair of transmission lines. Terminal T^M_{top} is not connected to any coil. An NFC tag is attached close to the conductor coil of a half relay so that the tag can be detected by the coil when the relay is connected to the reader, as displayed in Figure 4d. A brick placed on the nth layer can be detected by the station terminal T^n_{top} under it (through terminal T^1_{top} of the $n-1$th layer).

4.3.2 Box. A box (Figure 6) is an identifiable stackable unit based on the near-field relay method; therefore, it satisfies the D_{conn} requirement without requiring any electromechanical connection (i.e., magnetic connectors). Similar to the brick design, each box consists of N terminals. The box terminal number N is determined on the basis of D_{form} and can be different from the number of terminals on the brick and station (M). In a box, one terminal T is located on the top surface (T^i_{top}), and one terminal is located on the bottom surface (T^i_{bottom}), where $1 \le i \le N$. A total of $N-1$ relays

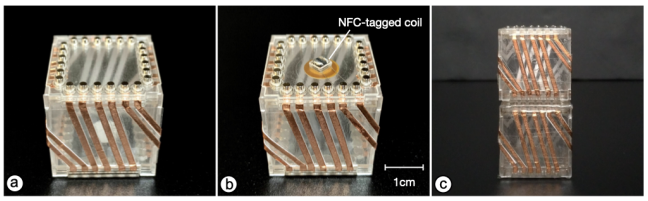

Figure 5: Images of bricks: (a) top view, (b) bottom view, and (c) two stacked bricks.

(r_j) are used to connect T^j_{top} and T^{j+1}_{bottom}, where $1 \le j \le N-1$. An NFC tag is attached to T^1_{bottom} so that a box placed on the nth layer can be detected by station terminal T^n_{top} under it (through the T^1_{top} conductor coil of the $n-1$-layer box).

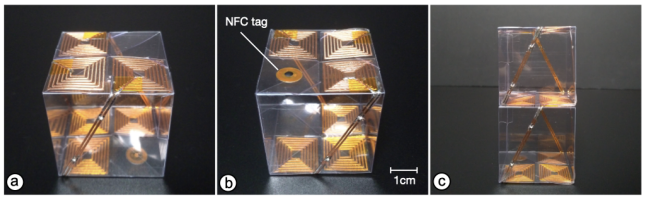

Figure 6: Box: (a) top view; (b) bottom view; (c) a box stacking on another box.

4.3.3 Adapter. An adapter (Figure 7) is an identifiable stackable unit for bridging a brick and box; therefore, the bottom side of an adapter is similar to a brick, and the top side of an adapter is similar to a box. The bottom side of an N-way adapter consists of $N+1$ pairs of magnetic connectors as terminals (T^i_{bottom}), where $1 \le i \le N+1$. Terminal T^1_{bottom} is connected to a conductor coil at the center of the box's bottom surface through a pair of transmission lines. An NFC tag is attached close to the coil so that the tag can be detected by the coil when the antenna is connected to the reader. The rest of the terminal T^i_{bottom}, where $2 \le i \le N+1$, is connected to the half relay at $T^{(i-1)}_{top}$.

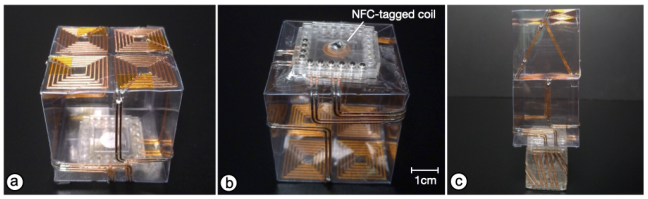

Figure 7: Images of an adapter: (a) top view, (b) bottom view, and (c) an adapter acting as an interface between a brick and a box.

4.4 Stacking Building Blocks on Stations

Bricks for Construction. Bricks are suitable for building stable structures that can sustain the state even when the station is held

in the hand. Figure 8a depicts 12-terminal bricks ($M = 12$) stacked in the same direction. The antenna circuitry aggregates signals from the top of all brick layers to the different multiplexer channels in the station. Alignment between every pair of adjacent bricks is guaranteed by the magnetic connectors, which are placed on the top and bottom of the brick as well as the top of the station. Consequently, each brick can be identified by the reader antenna, and the stacking height h of the bricks is determined by identifying which multiplexer channel i detects the tag, where $1 \leq i \leq M$. In this case, the maximum stacking height h_{max} is M.

Figure 8b displays a set of stacked bricks that are rotated with respect to each other. The orientation θ and stack height h of each brick can be resolved using the following equationswhen the multiplexer's channel i detected the tag: $\theta = \frac{\pi}{2}\lfloor i/4 \rfloor$ and $h = (i \bmod 4)+1$. In this case, the maximum stacking height (h_{max}) is $M/4$.

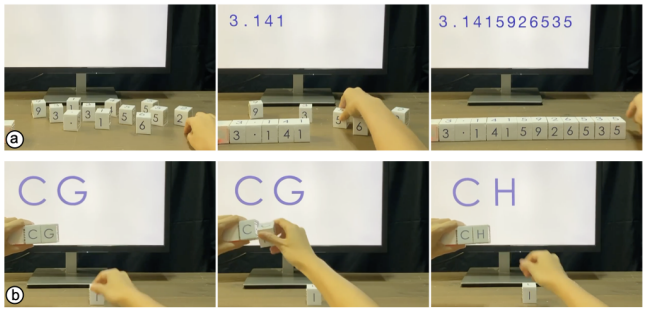

Figure 8: Stacking bricks on a station: (a) without rotation and (b) with rotation.

Adapter. An N-way Adapter is used to add N terminals to the top of a brick stack for reading NFC tags. When an N-way adapter is stacked on the ith layer, the identity of the adapter can be determined by the reader antenna from the multiplexer channel i. Furthermore, the N terminals located on the top, T^j_{top}, $1 \leq j \leq N$, serve as extensions of the next N multiplexer channels $(i + j)$ for detecting and identifying an NFC tag in its near field when $i + j \leq M$, where M is the number of station terminals. Figure 9 shows the application of an adapter on a station and on a set of bricks stacked on a station. This adapter can be used for reading N NFC tags.

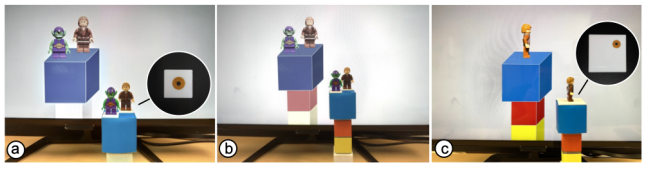

Figure 9: Adapter that converts the top of a stack into multiple NFC readers: (a) stacking an adapter on a station for sensing other NFC tags and (b) adding an adapter directly on a stack of bricks for (c) sensing the orientation of a tagged token.

Boxes for Interaction. Boxes are suitable for constructing interactive elements on an adapter because they enable frictionless operations. Figure 10b depicts four-terminal boxes stacked in the same direction on a N-way adapter. The identity of each brick can be determined by the reader antenna from a terminal of the adapter, and the stacking layer height h of the bricks is determined by identifying which multiplexer channel i detects the tag, where $1 \leq i \leq M$. In this case, the maximum height of box stacking is N.

Figure 10c displays a rotated box stacked on an adapter. The orientation θ and stack height h of each box can be determined using the following equations when the adapter's terminal j detected the tag: $\theta = \frac{\pi}{2}\lfloor j/4 \rfloor$ and $h = (j \bmod 4) + 1$. In this case, the maximum stacking height is $h_{max} = N/4$.

Figure 10a illustrates the application of N NFC tags on the top of the brick stack when the maximum stack height h_{max} is not reached. Even if the maximum height is reached, new NFC tags can still be read if the reader supports a multiread protocol and the ISO 15693 collision avoidance mechanism [10].

Figure 10: Stacking of boxes on an adapter stacked on a station: (a) sensing other NFC tags, (b) without rotation, and (c) with rotation.

4.5 Application Examples

Two simple cases are described in this section to illustrate how the three types of building blocks can be used in applications. Both cases indicate how NFCStack supports end-user customization (D_{cust}) due to the occlusion-free property of NFC.

Q & A. Figure 10 illustrates a word puzzle game. Several letter bricks and letter boxes are given to the users. One user (i.e., the questioner) stacks a sequence of bricks on one side and adds an adapter at the end to set the puzzle. Another user (i.e., the student) attempts to guess the sequence of boxes on the other side by switching boxes. When a box is in the correct position, the display shows the relevant character as feedback. When the student requires a hint, they can use an NFC token to observe the next character on the screen; however, the hint works only once for each quiz. The student then uses the remaining boxes to complete the answer.

Interactive Music Sequencer. Figure 11 displays an interactive music sequencer, which comprises many music note bricks, two adapters, and several instrument boxes. The user first stacks a sequence of notes on the station and then places an adapter on the stack to finalize it. Subsequently, the user stacks an instrument box, which contains one instrument on each of its four faces, on the adapter, and the note sequence starts looping the selected instrument. The user changes the instrument that will be used in the next loop by rotating the box. If he has constructed a second track with

another station, he can stack another instrument on the second stack to produce a chorus. The two tracks are in sync.

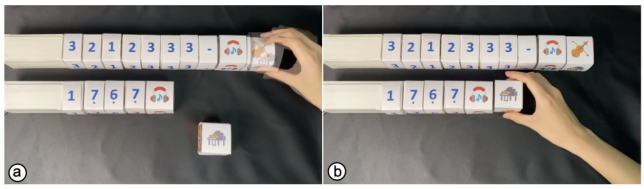

Figure 11: Interactive Music Sequencer: (a) selecting an instrument for the first track by rotating the box and (b) selecting an instrument for the second track.

4.6 Implementation

The constructed structures were implemented in accordance with the design considerations specified in Section 4.1. To satisfy the D_{form} requirement, the building blocks and stations had the form of graspable cubes or cuboids. To meet the $D_{material}$ requirement, the bricks and stations were fabricated from laser-cut acrylic sheets with a thickness of 1mm, whereas the adapters and boxes were fabricated from 0.25-mm-thick vinyl-cut polyethylene sheets. The conductors (transmission lines and coils) deployed on the surfaces of the bricks and stations were made from vinyl-cut copper foil. To satisfy the D_{elec} requirement, passive surface-mounted capacitors were used for regulating the coil's resonant frequency to the operating frequency range of NFC. These capacitors were arranged on the side of a building block or inside a station so that they did not impede stacking operations.

Station. Each of the $M = 12$ stations had dimensions of 30 (width; W) × 30 (Length; L) × 100 (height; H) mm^3 and supported a maximum of 12 layers of stacking. An RC522 NFC reader was used in each station. Without modifying the original hardware, we applied a half relay made of thin copper foil on top of the NFC reader's antenna so that we could obtain the NFC signal from the two terminals, as displayed in Figure 4b. To achieve a high coupling coefficient k, we aligned the coil with the center of the reader's antenna coil and made the dimensions of the half relay's conductor coil similar to those of the reader's antenna coil. The 0.47 uH conductor coil of the half relay contained six turns and had dimensions of 20 mm (diameter; ϕ) × 0.1 mm (thickness; T). This coil was wound with a 0.8-mm-wide of vinyl-cut copper trace, with the gap between adjacent parts of the trace being 0.6 mm, and a 300-pF surface-mounted parallel capacitor was used to tune the coil's resonant frequency ($f_0 \sim 13.56MHz$).

The top surface of a station was the same as the top surface of a brick and contained 12 pairs of magnetic connectors. The circuitry of the time-domain multiplexed NFC reader contained an off-the-shelf MFRC522 NFC reader, a 1:16 TI CD74HC4067 multiplexer, and an Arduino Pro Mini board. Tag events were captured using a microcontroller and then sent to the application through a serial connection. The NFC reader's read rate was set as 250 reads per second (rps); thus, each of the 12 terminals had an interactive read rate of approximately 20.5 rps. Each operation was detected with latency of less than 0.2 s.

4.6.1 *Building Blocks.*

Brick. Each of the $M = 12$ bricks had dimensions of 30 (W) × 30 (L) × 30 (H) mm^3. Moreover, each brick contained 12 pairs of magnetic connectors on both top and the bottom of the brick, three pairs per side. The magnetic connectors were convex N35 neodymium magnets whose bottom side had dimensions of 3 mm (ϕ) × 1 mm (T) and whose top side had dimensions of 2 mm (ϕ) × 2 mm (T). To extend the NFC read range, 11 pairs of transmission lines fabricated from 2-mm (W) copper tape, with the gaps between the lines being a 1.4-mm were deployed on each brick to connect the magnetic connectors. To meet the D_{conn} requirement, the identity of a brick was determined using an off-the-shelf 1.4 uH Bourn SDR0403-1R4ML unshielded inductor with dimensions of 4.5 mm (ϕ)× 3.2 mm (T). This inductor was attached to the bottom of a brick, and a 10 mm (ϕ) NTAG213 NFC tag was attached to the inductor. The small inductor (coil and tag) used was suitable for the bricks because physical alignment was guaranteed by the magnetic connectors.

Box. Each of the $N = 4$ boxes had dimensions of 45 (W) × 45 (L) × 45 (H) mm^3. The boxes were almost two times larger than the bricks but were still graspable by an adult hand. To meet the D_{conn} requirement, $N - 1 = 3$ vinyl-cut relays were deployed on the boxes. Each relay comprised two 6-turn, 20 mm (ϕ) × 0.1 mm (T), and 0.47-uH coils wound with a 0.8-mm-wide vinyl-cut copper trace, with a 0.6-mm gap between the trace; a 300-pF surface-mounted parallel capacitor; and a pair of transmission lines made of copper tape with a trace width of 0.8 mm and a gap of 0.5 mm. To determine the identity of a box, a 10-mm (ϕ) NTAG213 NFC tag was attached at the location T^M_{bottom}.

Adapter. Each $N = 4$-way adapter had the same top-surface configuration as the boxes and the same bottom-surface configuration as the bricks. A laser-cut frame used in the brick is attached to the bottom. Each adapter had a height of 45 mm.

5 USING BRICKS AND STATIONS FOR 2.5D CONSTRUCTION

With a one-dimensional or 2D array of stations, 1.5-dimensional (1.5D) or 2.5D rich-ID construction can be achieved with the bricks. Figure 12 depicts our prototype system, which supports 1.5D and 2.5D rich-ID construction with four stations. On the basis of the experimental results shown in Section 6.2.3, we increased the dimensions of the bricks from $30(W)mm \times 30(L)mm$ to $36(W)mm \times 36(L)mm$ by adding a 3-mm-thick acrylic shell to each brick, as shown in Figure 13a. The height of the bricks was unchanged. For the bricks and stations with a shell, the $d_{station}$ value was maintained as 6mm. The bricks and stations were still sufficiently small to be grasped between the fingers (D_{form}). A one-way adapter (Figure 13b) could be used to convert the top of each stack or station into a portal for sensing NFC-tagged tokens.

Identifying the Relative Positions of Stations. Identification of the relative positions of stations enables stations to be stacked in various directions and therefore facilitates batch operations by enabling manipulation of the entire stack, as demonstrated in [29]. To determine a station's relative position with high resolution, we

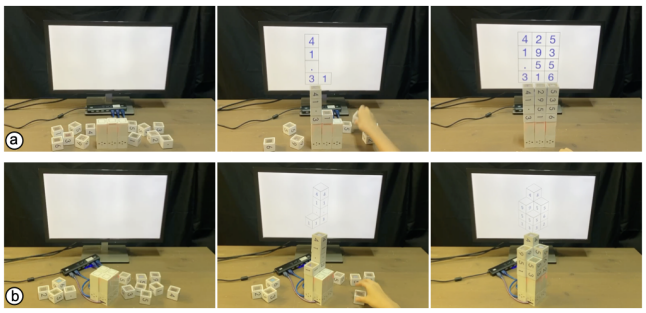

Figure 12: Constructions on tiled stations: (a) 1.5D construction on a 1x3 array of stations and (b) 2.5D construction on a 2×2 array of stations.

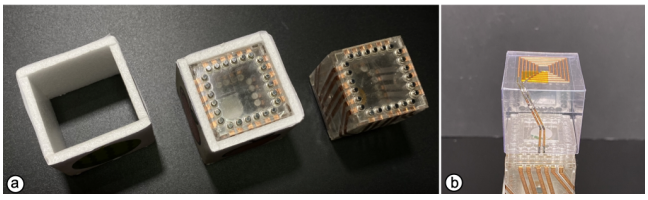

Figure 13: Hardware adaptation for tiling stations: (a) bricks with an additional shell that maintains the distance between bricks on the neighboring station and (b) a one-way adapter.

used an additional NFC tag-antenna coil pair on the surface of each of the four sides of the stations (Figures 14a and 14b). With these four additional multiplexer channels, each of the 16 terminals achieved an interactive read rate of approximately 15.6 rps. Each coil was connected to a multiplexer channel through transmission lines. Each tag was placed sufficiently far from the coil next to it to ensure that the tag was not detected accidentally. Once one station had connected to another, the two corresponding antenna coils became activated simultaneously and read each other's tag. The two stations recognized each other's ID, and the system inferred the topology from the information.

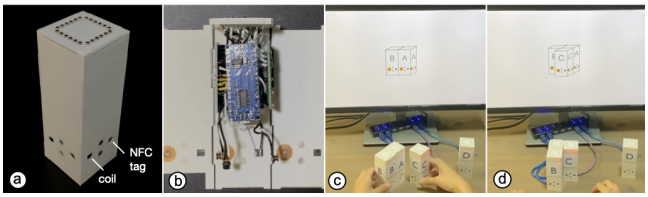

Figure 14: Tileable stations: (a) additional pairs of tag and coil are added on each side; (b) signal processing unit; (c-d) stacking stations side by side.

Application Example. Figure 15 depicts a tangible Scratch-to-Python programming user interface, which was implemented using the Blockly JavaScript application programming interface (API) [5] and Web Serial API [6]. This programming interface consisted of a 1x4 array of stations for user interaction. In the programming application, lines of code were stacked using meta bricks, which which contained a slot filled with parameter bricks and implemented a specific function (e.g., the for-loop function) or control logic. When a user stacked lines of code, the computer display showed the digital representation of the lines of code, which was the same as the corresponding physical representation. The as-direct-as-possible mapping between the blocks and the Scratch as well as the Python code was shown to the user immediately after each operation, which was possible because NFCStack resolves the concurrent stacking events of bricks.

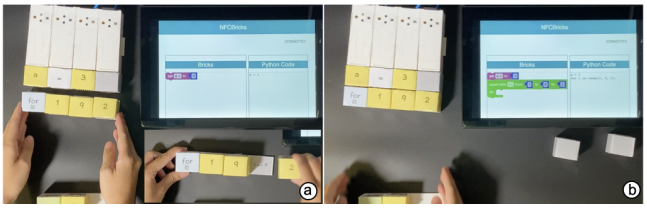

Figure 15: Addition of a line of code by a user in a tangible programming application, by using a meta brick, which consists of a slot filled with parameter bricks.

Supporting Frictionless Tangible Interactions for 2.5D Construction. Although the adopted four-way adapters and $N = 4$ boxes were larger than the adopted bricks, we made these parts compatible with a 2.5D system by simply thickening the shell of each brick and station to fit the size of boxes while meeting the $d_{station}$ requirement (Figure 10). By using a larger (e.g., 3×5) grid of deployed NFCStack stations, the tangible Minecraft applications in RFIBricks [17] can be implemented with a considerably smaller form factor without being dependent on an external reader, thereby supporting simultaneous interactions among multiple users and enbling frictionless inputs with the Boxes. Ultimately, we envision that tangible interaction with the boxes on such a station can be as easy as throwing an inflatable dice.

6 SYSTEM EVALUATION

A series of studies were conducted to understand whether the proposed system's performance satisfied our design objectives related to reliable electrical connection (D_{conn}),

6.1 Performance of the Adopted Antenna Extension Methods

In the first study, we investigated the performance of the adopted antenna extension methods after stacking.

Apparatus. A NanoVNA v2 vector network analyzer (VNA) and standard 50-Ω SMA connectors were used to conduct measurements (Figure 16). A total of 12 boxes and 12 relays, which are the same as what we used in the boxes, were used in the test. For measuring the bricks, channel 1 of the VNA was connected to the bricks through a pair of magnetic connectors. For measuring the relays, a coil

[5] https://developers.google.com/blockly

[6] https://wicg.github.io/serial

extender with the same specifications as the coil extender in the stations was connected to channel 1 of the VNA. An NFC tag with the same specifications as those used in the building boxes, was connected to channel 2 of the VNA.

Procedure. Each measurement was performed after a box was stacked on a station. We connected the antenna's terminals to the port of the VNA by using an SMA connector and measured the antenna's S11 return loss and S21 power between 10.92 and 16.2 MHz. We conducted five 5 measurements, discarded the two outliers, and averaged the remaining three measurements. Twelve results were collected for 1-12 layers of box and brick stacking.

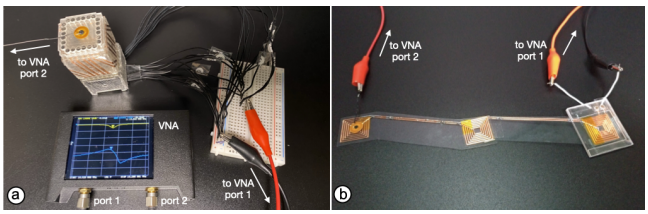

Figure 16: Experimental apparatus for evaluating antenna extension performance: (a) example settings for S11 measurement (with a brick and tagged coil; layer 2) and (b) example settings for S21 measurement (with two relays and a tag; layer 3).

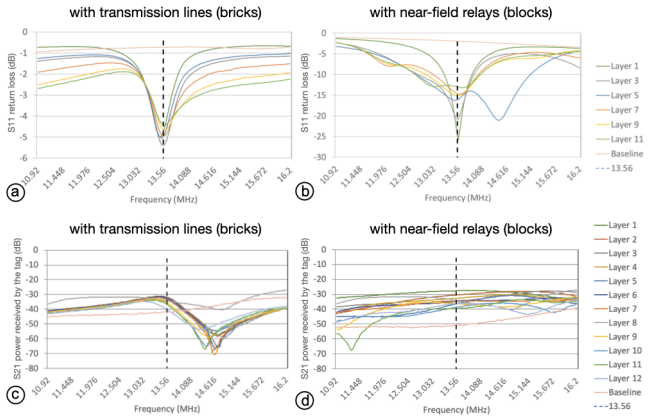

Figure 17: Performance of the antenna extension methods: (a) S11 measurements when using transmission line extension, (b) S11 measurements when using multihop extension, (c) S21 measurements when using transmission line extension, and (d) S21 measurements when using multihop extension.

Results. Figure 17 shows the S11 and S21 measurements. The S11 measurements represent the reflected power that the VNA attempted to deliver to the antenna through port 1 connected to the reader, and the S21 measurements represent the power transferred from the reader to the tag connected to port 2; these results indicate whether the tag received sufficient power (i.e., -48*dBi*) during operation. Only the results for the stacking of odd numbers of layers are displayed in Figure 17 to enable clear visualization.

The S11 measurements indicated that impedance matching was achieved between the power source and the inductor at 13.56 MHz when using the transmission line extension and multihop extension methods, regardless of the height of the brick stacking or the number of relay connections. This finding indicates the effectiveness of the aforementioned methods. The S11 return loss observed when using the multihop extension method was greater than that observed when using the transmission line extension method, which indicated that more power was radiated or absorbed as loss within the antenna when the multihop extension method was used.

The S21 measurements indicated that the NFC tag received sufficient energy at 13.56 MHz, regardless of the height of the brick stacking or the number of relay connections. Except for the S21 measurements for the 12th brick layer, all S21 measurements were higher than the baseline value for the condition in which the tag did not receive any signal. Therefore, the two adopted antenna extension methods are effective.

6.2 Stacking Performance

In the second study, we investigated the sensing capability of the system stack in three measurement sessions.

6.2.1 *Session 1: Full Stack on One Station.*

Apparatus. Twelve bricks, one adapter, four boxes, and one station were used for the measurement.

Procedure. We randomly selected one brick from the pool of boxes and stacked the selected box on the station. We then performed forty-five 3-s reads of every NFC tag on the station. If more than 95% (=43) of the reads of all the tags on two stations were successful, we stacked another brick, adapter, or box layer on the station and performed additional 3-s reads until the reads did not meet the success criterion or reached the 12-layer height limit. Two extreme conditions were tested: (1) a stack of 12 bricks and (2) a stack of 7 bricks, 1 adapter, and 4 boxes in sequence. Five iterations were performed for each measurement.

Results. The station passed the full-stack test in all five iterations under the aforementioned two extreme conditions, which indicated that the proposed system reliably handled the stacking of the three types of building blocks in a single station setting.

6.2.2 *Session 2: Effect of Offsets between Boxes on Box Stacking.*

In the second session, we investigated how the boxes' stacking performance was affected by misalignment between boxes. As discussed in Section 3.1, offsets between coils, which cause a decrease in the coupling factor, affect the power transfer efficiency.

Apparatus. As in session 1, 12 bricks, 1 adapter, 4 boxes, and 1 station were used for the measurements in session 2; however, only the 4 boxes were changed for testing in session 2. A few 2-mm-thick acrylic sheets were used as spacers to maintain the offset distances between two boxes, as shown in Figure 18a.

Procedure. Two initial conditions were considered: 1) a stack of only one adapter, which represents the easiest condition, and 2) a stack of a sequence of seven bricks and one adapter, which represents the most difficult condition. Under each condition, we used the same procedures as those used in session 1. Each box layer

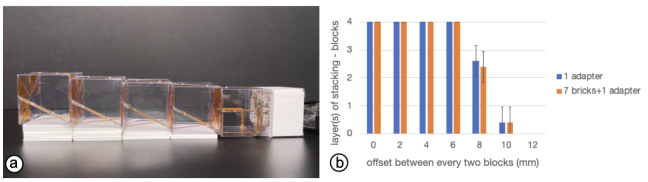

Figure 18: Effect of the offsets between boxes on box stacking: (a) experimental apparatus (x = 4mm) and (b) experimental results.

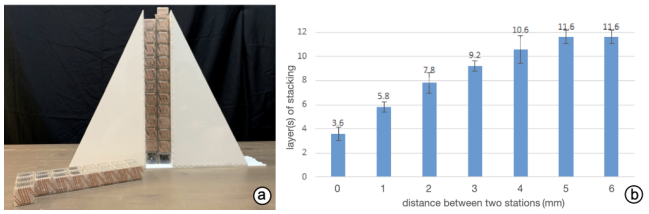

Figure 19: Effect of station distance on brick stacking: (a) experimental apparatus and (b) experimental results.

was added to the station with an x-mm offset against the box or adapter in the previous layer, and 3-s reads were performed until the reads did not meet the success criteria or the four-layer height limit was reached. Seven distances between $d_{station}$ = 0 and 12 mm (in 2-mm steps) were considered in the measurements. Five iterations were performed for each offset.

Results. Figure 18b displays the experimental results obtained in session 2. The station passed the full-stack test in all five iterations under the aforementioned two extreme conditions when $x \leq 6mm$, which indicates that the developed system reliably handles the stacking of boxes with a slight offset. Moreover, when the stack could only resolve M = 2.6 layers (SD) and 2.4 layers (SD) under conditions 1 and 2, respectively, under an x value of 8mm, it became difficult to stack the boxes vertically for more than two layers without stack collapsing. Therefore, the developed system can support basic usage and withstand frictionless stacking.

6.2.3 Session 3: Effect of Station Distance on Brick Stacking. In the third session, we investigated how the brick stacking performance was affected by the distance between two stations because proximity between neighboring transmission lines may affect the performance of NFC sensing.

Apparatus. Twenty-four bricks and two stations were used for the measurements in session 3. Boxes and adapters were not used in this session because they were larger than the stations. A few 1-mm-thick acrylic sheets were used as spacers to maintain the distance between the stacks, as displayed in Figure 19a.

Procedure. The measurement procedure adopted in session 3 was similar to that used in session 1. Two boxes were added to each station and 3-s reads were performed until the reads did not meet the success criterion or the 12-layer height limit was reached. Seven distances ($d_{station}$) between 0 and 6 mm (1-mm steps) were considered in the measurements. Five iterations were performed for each distance.

Results. Figure 19b shows the results obtained in session 3. The brick's stack height (M) increased from 3.6 layers (SD = 0.55 layers) when $d_{station}$ was 0mm to 11.6 layers (SD = 0.55 layers) when $d_{station}$ was 5mm and 6mm. Although the two stations did not pass the full-stack test in two out of the five iterations when $d_{station}$ was 5 or 6mm, at least 11 layers of reliable brick stacking were achieved for the two stations in all the iterations.

7 DISCUSSION

Applications and Contribution. Many applications of Rich-ID building blocks have been proposed in the previous work, such as 3D modeling [1–3], physical computing [20], tangible programming (see the overview in [32]), gaming [29, 33], and context construction [13, 29, 36]. Tangible user interfaces have applications in the education and entertainment domains. A new application of these blocks is not proposed in this paper. Instead, we focused on a technical contribution, namely the design of a passive rich-ID building block system that enables frictionless NFC-based tangible interaction. This paper describes the functioning of the designed system by using simple examples. The performance of the designed system was evaluated by conducting experiments. The results of the present study can act as a reference to help researchers construct and extend building block systems. Users can employ the techniques and hardware platform developed in this research to enrich and customize their applications. An extension of the present study can include organizing design workshops to collect additional information on artifacts and design processes.

User Involvement in Evaluation. The repeated measurements obtained in session 2 (Section 5.2.2) suggest that reliable block detection is achieved with the proposed system when the offset x≤6mm. Because NFC is unaffected by the human body, this result indicates that the developed system provides an user experience without strict alignment between parts being required. Future studies can obtain user feedback (e.g., through usability testing and cocreation workshops) to improve the system designed in this study.

Multiplexing vs. System Performance. The multiplexer used in each station in this paper had a resistance of approximately 70 Ω, which decreased our RLC circuit's quality factor (Q) to 1.7. Although a circuit with $Q \geq 1$ is compatible with NFC, such a circuit negatively affects the performance of relay-based extension. We conducted a full-stack experiment with relays under the same setting depicted in Figure 16b by using the procedure described in Section 5.2.1 to determine the number of relay connections that allowed a reader to read a tag with and without the multiplexer. The results indicated that the tag could be read after 12 and 7 connections without and with the multiplexer, respectively. We provide two suggestions for future research. First, researchers can use multiple NFC readers instead of a multiplexer so that no additional resistance R_{mux} is generated in the RLC circuit. Software-defined multiplexing, such as selecting only one NFC at a time by using

the Serial Peripheral Interface (SPI) protocol, can be used to prevent crosstalk. Second, low-ohmic multiplexers can be employed to increase the RLC antenna's Q-factor.

Rich interactivity. Input and output modalities can be added more easily to the NFCStack system than to UHF RFID building block systems [29] and the NFC Stackers in the Zanzibar system [41]. Some terminals of the NFCStack system can be directly connected to the general-purpose input and output (GPIO) pins of a microcontroller to enable building blocks to interface with additional sensors (e.g., motion sensors), displays (e.g., organic light-emitting diode displays [OLED]), and actuators (e.g., servo motors). These terminals can be added to the center of the building blocks, so they do not necessarily compromise the stacking capability. Moreover, we suggest keeping the additional data and power lines sufficiently far away from the surface NFC antennas and transmission lines to prevent these lines from interfering with stack sensing and recognition.

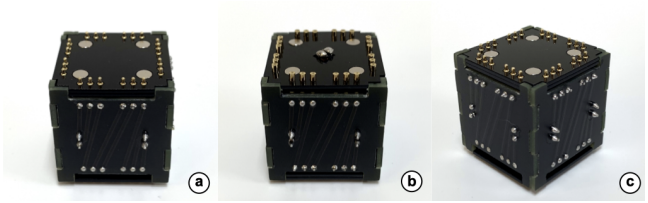

Figure 20: Brick made of printed circuit boards and pogo pins: (a) top view, (b) bottom view, and (c) side view.

Durability and Scalability. Although the developed system supports personal fabrication, its durability and scalability are limited because it is made of vinyl-cut copper circuitry and plastic. To enhance the electromechanical and mechanical durability of the developed system, a semiautomated printed circuit board assembly (PCBA) and standard connectors should be used. Figure 20 displays an example of a PCBA implementation of bricks. This assembly comprises four PCB boards and standard POGO pins, which can be reliably soldered onto these boards to enhance the system's durability. We also suggest producing boxes with a flexible PCB to replace the vinyl-cut parts of the current system. PCBA fabrication reduces human error and the effort needed for manual assembly and would therefore facilitate deployment at scale.

Waterproof and Dustproof. NFC is an occlusion-free and dustproof technology. Operating at 13.56 MHz, NFC is not strongly affected by water [10]. Therefore, if a station with an adapter mounted on its top has a water-tight seal, it can detect a stack of boxes if each of them also has a water-tight seal. By mounting a magnet inside each box and adapter-mounted station, they can also support sturdy construction as bricks do. A waterproof and dustproof NFCStack system would be larger than the one proposed in this paper because the size of the box depends on the size of the coils. Nevertheless, a waterproof and dustproof NFCStack system has high potential for use in the development of child-friendly tangible kits.

8 CONCLUSION

This paper describes NFCStack, which is an NFC-based physical building block system that supports stacking and frictionless interaction. The system contains three types of building block: bricks, boxes, and adapters. These blocks can handle concurrent stack events and facilitate the development of an NFC system that enables physical construction and tangible interaction. Evaluation results obtained when implementing the proposed system indicated the effectiveness of this system. This paper also presents preliminary results obtained in generalized applications of the NFCStack system. The results of this study can act as a reference for future research on stacking systems.

ACKNOWLEDGMENTS

We acknowledge Associate Chairs and the anonymous reviewers for their insightful comments. This research was supported in part by the Ministry of Science and Technology of Taiwan (MOST 110-2634-F-002-051, 110-2218-E-002-025), National Taiwan University.

REFERENCES

[1] Robert Aish, James L. Frankel, John H. Frazer, and Anthony T. Patera. 2001. Computational Construction Kits for Geometric Modeling and Design (Panel Abstract). In *Proceedings of the 2001 Symposium on Interactive 3D Graphics (I3D '01)*. Association for Computing Machinery, New York, NY, USA, 125–128. https://doi.org/10.1145/364338.364379

[2] Roslyn R Aish. 1981. Modelling arrangements. US Patent 4,275,449.

[3] David Anderson, James L. Frankel, Joe Marks, Darren Leigh, Eddie Sullivan, Jonathan Yedidia, and Kathy Ryall. 1999. Building Virtual Structures with Physical Blocks. In *Proceedings of the 12th Annual ACM Symposium on User Interface Software and Technology* (Asheville, North Carolina, USA) *(UIST '99)*. ACM, New York, NY, USA, 71–72. https://doi.org/10.1145/320719.322587

[4] Masahiro Ando, Yuichi Itoh, Toshiki Hosoi, Kazuki Takashima, Kosuke Nakajima, and Yoshifumi Kitamura. 2014. StackBlock: Block-shaped Interface for Flexible Stacking. In *Proceedings of the Adjunct Publication of the 27th Annual ACM Symposium on User Interface Software and Technology* (Honolulu, Hawaii, USA) *(UIST'14 Adjunct)*. ACM, New York, NY, USA, 41–42. https://doi.org/10.1145/2658779.2659104

[5] Daniel Avrahami and Scott E. Hudson. 2002. Forming Interactivity: A Tool for Rapid Prototyping of Physical Interactive Products. In *Proceedings of the 4th Conference on Designing Interactive Systems: Processes, Practices, Methods, and Techniques* (London, England) *(DIS '02)*. Association for Computing Machinery, New York, NY, USA, 141–146. https://doi.org/10.1145/778712.778735

[6] Maribeth Back, Jonathan Cohen, Rich Gold, Steve Harrison, and Scott Minneman. 2001. Listen Reader: An Electronically Augmented Paper-Based Book. In *Proceedings of the SIGCHI Conference on Human Factors in Computing Systems* (Seattle, Washington, USA) *(CHI '01)*. Association for Computing Machinery, New York, NY, USA, 23–29. https://doi.org/10.1145/365024.365031

[7] Tom Bartindale and Chris Harrison. 2009. Stacks on the Surface: Resolving Physical Order Using Fiducial Markers with Structured Transparency. In *Proceedings of the ACM International Conference on Interactive Tabletops and Surfaces* (Banff, Alberta, Canada) *(ITS '09)*. ACM, New York, NY, USA, 57–60. https://doi.org/10.1145/1731903.1731916

[8] Patrick Baudisch, Torsten Becker, and Frederik Rudeck. 2010. Lumino: Tangible Blocks for Tabletop Computers Based on Glass Fiber Bundles. In *ACM CHI 2010 Conference Proceedings* (Atlanta, Georgia, USA). 1165–1174.

[9] Liwei Chan, Stefanie Müller, Anne Roudaut, and Patrick Baudisch. 2012. CapStones and ZebraWidgets: Sensing Stacks of Building Blocks, Dials and Sliders on Capacitive Touch Screens. In *ACM CHI 2012 Conference Proceedings* (Austin, Texas, USA). 2189–2192.

[10] Klaus Finkenzeller. 2003. *RFID Handbook: Fundamentals and Applications in Contactless Smart Cards and Identification* (2nd ed.). Wiley Publishing.

[11] Baptiste Garnier, Philippe Mariage, François Rault, Cédric Cochrane, and Vladan Koncar. 2021. Electronic-components less fully textile multiple resonant combiners for body-centric near field communication. *Scientific Reports* 11, 1 (25 Jan 2021), 2159. https://doi.org/10.1038/s41598-021-81246-z

[12] Audrey Girouard, Aneesh Tarun, and Roel Vertegaal. 2012. DisplayStacks: Interaction Techniques for Stacks of Flexible Thin-film Displays. In *Proceedings of the SIGCHI Conference on Human Factors in Computing Systems* (Austin, Texas, USA) *(CHI '12)*. ACM, New York, NY, USA, 2431–2440. https://doi.org/10.1145/2207676.2208406

[13] Alix Goguey, Cameron Steer, Andrés Lucero, Laurence Nigay, Deepak Ranjan Sahoo, Céline Coutrix, Anne Roudaut, Sriram Subramanian, Yutaka Tokuda, Timothy Neate, Jennifer Pearson, Simon Robinson, and Matt Jones. 2019. PickCells: A Physically Reconfigurable Cell-composed Touchscreen. In *Proceedings of the 2019 CHI Conference on Human Factors in Computing Systems* (Glasgow, Scotland Uk) *(CHI '19)*. ACM, New York, NY, USA, Article 273, 14 pages. https://doi.org/10.1145/3290605.3300503

[14] Matthew G. Gorbet, Maggie Orth, and Hiroshi Ishii. 1998. Triangles: Tangible Interface for Manipulation and Exploration of Digital Information Topography. In *Proceedings of the SIGCHI Conference on Human Factors in Computing Systems* (Los Angeles, California, USA) *(CHI '98)*. ACM Press/Addison-Wesley Publishing Co., USA, 49–56. https://doi.org/10.1145/274644.274652

[15] Jason T. Griffin, Steven Henry Fyke, Christopher Lyle Bender, Santiago Carbonell Duque, David Ryan Walker, and Jerome Pasquero. 2014. Near-field communication (NFC) system providing mobile wireless communications device operations based upon timing and sequence of NFC sensor communication and related methods. U.S. Patent 8,670,709.

[16] Toshiki Hosoi, Kazuki Takashima, Tomoaki Adachi, Yuichi Itoh, and Yoshifumi Kitamura. 2014. A-blocks: Recognizing and Assessing Child Building Processes During Play with Toy Blocks. In *SIGGRAPH Asia 2014 Emerging Technologies* (Shenzhen, China) *(SA '14)*. ACM, New York, NY, USA, Article 1, 2 pages. https://doi.org/10.1145/2669047.2669061

[17] Meng-Ju Hsieh, Rong-Hao Liang, Da-Yuan Huang, Jheng-You Ke, and Bing-Yu Chen. 2018. RFIBricks: Interactive Building Blocks Based on RFID. In *Proceedings of the 2018 CHI Conference on Human Factors in Computing Systems* (Montreal QC, Canada) *(CHI '18)*. Association for Computing Machinery, New York, NY, USA, 1–10. https://doi.org/10.1145/3173574.3173763

[18] Hiroshi Ishii and Brygg Ullmer. 1997. Tangible Bits: Towards Seamless Interfaces Between People, Bits and Atoms. In *Proceedings of the ACM SIGCHI Conference on Human Factors in Computing Systems* (Atlanta, Georgia, USA) *(CHI '97)*. ACM, New York, NY, USA, 234–241. https://doi.org/10.1145/258549.258715

[19] Robert J.K. Jacob, Audrey Girouard, Leanne M. Hirshfield, Michael S. Horn, Orit Shaer, Erin Treacy Solovey, and Jamie Zigelbaum. 2008. Reality-Based Interaction: A Framework for Post-WIMP Interfaces. In *Proceedings of the SIGCHI Conference on Human Factors in Computing Systems* (Florence, Italy) *(CHI '08)*. Association for Computing Machinery, New York, NY, USA, 201–210. https://doi.org/10.1145/1357054.1357089

[20] Yoshifumi Kitamura, Yuichi Itoh, and Fumio Kishino. 2001. Real-Time 3D Interaction with ActiveCube. In *CHI '01 Extended Abstracts on Human Factors in Computing Systems* (Seattle, Washington) *(CHI EA '01)*. Association for Computing Machinery, New York, NY, USA, 355–356. https://doi.org/10.1145/634067.634277

[21] Jinha Lee, Yasuaki Kakehi, and Takeshi Naemura. 2009. Bloxels: Glowing Blocks as Volumetric Pixels. In *ACM SIGGRAPH 2009 Emerging Technologies* (New Orleans, Louisiana) *(SIGGRAPH '09)*. Association for Computing Machinery, New York, NY, USA, Article 5, 1 pages. https://doi.org/10.1145/1597956.1597961

[22] Jakob Leitner and Michael Haller. 2011. Geckos: Combining Magnets and Pressure Images to Enable New Tangible-object Design and Interaction. In *Proceedings of the SIGCHI Conference on Human Factors in Computing Systems* (Vancouver, BC, Canada) *(CHI '11)*. ACM, New York, NY, USA, 2985–2994. https://doi.org/10.1145/1978942.1979385

[23] Hanchuan Li, Eric Brockmeyer, Elizabeth J. Carter, Josh Fromm, Scott E. Hudson, Shwetak N. Patel, and Alanson Sample. 2016. PaperID: A Technique for Drawing Functional Battery-Free Wireless Interfaces on Paper. In *Proceedings of the 2016 CHI Conference on Human Factors in Computing Systems* (San Jose, California, USA) *(CHI '16)*. Association for Computing Machinery, New York, NY, USA, 5885–5896. https://doi.org/10.1145/2858036.2858249

[24] Rong-Hao Liang, Liwei Chan, Hung-Yu Tseng, Han-Chih Kuo, Da-Yuan Huang, De-Nian Yang, and Bing-Yu Chen. 2014. GaussBricks: Magnetic Building Blocks for Constructive Tangible Interactions on Portable Displays. In *Proceedings of the SIGCHI Conference on Human Factors in Computing Systems* (Toronto, Ontario, Canada) *(CHI '14)*. Association for Computing Machinery, New York, NY, USA, 3153–3162. https://doi.org/10.1145/2556288.2557105

[25] Rong-Hao Liang and Zengrong Guo. 2021. *NFCSense: Data-Defined Rich-ID Motion Sensing for Fluent Tangible Interaction Using a Commodity NFC Reader*. Association for Computing Machinery, New York, NY, USA. https://doi.org/10.1145/3411764.3445214

[26] Rong-Hao Liang, Meng-Ju Hsieh, Jheng-You Ke, Jr-Ling Guo, and Bing-Yu Chen. 2018. RFIMatch: Distributed Batteryless Near-Field Identification Using RFID-Tagged Magnet-Biased Reed Switches. In *Proceedings of the 31st Annual ACM Symposium on User Interface Software and Technology* (Berlin, Germany) *(UIST '18)*. Association for Computing Machinery, New York, NY, USA, 473–483. https://doi.org/10.1145/3242587.3242620

[27] Rong-Hao Liang, Han-Chih Kuo, Liwei Chan, De-Nian Yang, and Bing-Yu Chen. 2014. GaussStones: Shielded Magnetic Tangibles for Multi-Token Interactions on Portable Displays. In *Proceedings of the 27th Annual ACM Symposium on User Interface Software and Technology* (Honolulu, Hawaii, USA) *(UIST '14)*. Association for Computing Machinery, New York, NY, USA, 365–372. https://doi.org/10.1145/2642918.2647384

[28] Rongzhou Lin, Han-Joon Kim, Sippanat Achavananthadith, Selman A. Kurt, Shawn C. C. Tan, Haicheng Yao, Benjamin C. K. Tee, Jason K. W. Lee, and John S. Ho. 2020. Wireless battery-free body sensor networks using near-field-enabled clothing. *Nature Communications* 11, 1 (23 Jan 2020), 444. https://doi.org/10.1038/s41467-020-14311-2

[29] Chin-Yuan Lu, Han-Wei Hsieh, Rong-Hao Liang, Chi-Jung Lee, Ling-Chien Yang, Mengru Xue, Jr-Ling Guo, Meng-Ju Hsieh, and Bing-Yu Chen. 2021. *Combining Touchscreens with Passive Rich-ID Building Blocks to Support Context Construction in Touchscreen Interactions*. Association for Computing Machinery, New York, NY, USA. https://doi.org/10.1145/3411764.3445722

[30] Thomas W. Malone. 1983. How Do People Organize Their Desks?: Implications for the Design of Office Information Systems. *ACM Trans. Inf. Syst.* 1, 1 (Jan. 1983), 99–112. https://doi.org/10.1145/357423.357430

[31] Einar Sneve Martinussen and Timo Arnall. 2009. Designing with RFID. In *Proceedings of the 3rd International Conference on Tangible and Embedded Interaction* (Cambridge, United Kingdom) *(TEI '09)*. Association for Computing Machinery, New York, NY, USA, 343–350. https://doi.org/10.1145/1517664.1517734

[32] Timothy S McNerney. 2004. From turtles to Tangible Programming Bricks: explorations in physical language design. *Personal and Ubiquitous Computing* 8, 5 (2004), 326–337.

[33] David Merrill, Jeevan Kalanithi, and Pattie Maes. 2007. Siftables: Towards Sensor Network User Interfaces. In *Proceedings of the 1st International Conference on Tangible and Embedded Interaction* (Baton Rouge, Louisiana) *(TEI '07)*. ACM, New York, NY, USA, 75–78. https://doi.org/10.1145/1226969.1226984

[34] Farshid Salemi Parizi, Eric Whitmire, and Shwetak Patel. 2019. AuraRing: Precise Electromagnetic Finger Tracking. *Proc. ACM Interact. Mob. Wearable Ubiquitous Technol.* 3, 4, Article 150 (dec 2019), 28 pages. https://doi.org/10.1145/3369831

[35] Amanda Parkes and Hiroshi Ishii. 2010. Bosu: A Physical Programmable Design Tool for Transformability with Soft Mechanics. In *Proceedings of the 8th ACM Conference on Designing Interactive Systems* (Aarhus, Denmark) *(DIS '10)*. Association for Computing Machinery, New York, NY, USA, 189–198. https://doi.org/10.1145/1858171.1858205

[36] Florian Perteneder, Kathrin Probst, Joanne Leong, Sebastian Gassler, Christian Rendl, Patrick Parzer, Katharina Fluch, Sophie Gahleitner, Sean Follmer, Hideki Koike, and Michael Haller. 2020. Foxels: Build Your Own Smart Furniture. In *Proceedings of the Fourteenth International Conference on Tangible, Embedded, and Embodied Interaction* (Sydney NSW, Australia) *(TEI '20)*. Association for Computing Machinery, New York, NY, USA, 111–122. https://doi.org/10.1145/3374920.3374935

[37] Hayes Solos Raffle, Amanda J. Parkes, and Hiroshi Ishii. 2004. *Topobo: A Constructive Assembly System with Kinetic Memory*. Association for Computing Machinery, New York, NY, USA, 647–654. https://doi.org/10.1145/985692.985774

[38] Jun Rekimoto, Brygg Ullmer, and Haruo Oba. 2001. DataTiles: A Modular Platform for Mixed Physical and Graphical Interactions. In *Proceedings of the SIGCHI Conference on Human Factors in Computing Systems* (Seattle, Washington, USA) *(CHI '01)*. ACM, New York, NY, USA, 269–276. https://doi.org/10.1145/365024.365115

[39] Ryo Takahashi, Masaaki Fukumoto, Changyo Han, Takuya Sasatani, Yoshiaki Narusue, and Yoshihiro Kawahara. 2020. *TelemetRing: A Batteryless and Wireless Ring-Shaped Keyboard Using Passive Inductive Telemetry*. Association for Computing Machinery, New York, NY, USA, 1161–1168. https://doi.org/10.1145/3379337.3415873

[40] Brygg Ullmer, Hiroshi Ishii, and Robert J. K. Jacob. 2005. Token+constraint Systems for Tangible Interaction with Digital Information. *ACM Trans. Comput.-Hum. Interact.* 12, 1 (March 2005), 81–118. https://doi.org/10.1145/1057237.1057242

[41] Nicolas Villar, Daniel Cletheroe, Greg Saul, Christian Holz, Tim Regan, Oscar Salandin, Misha Sra, Hui-Shyong Yeo, William Field, and Haiyan Zhang. 2018. Project Zanzibar: A Portable and Flexible Tangible Interaction Platform. In *Proceedings of the 2018 CHI Conference on Human Factors in Computing Systems* (Montreal QC, Canada) *(CHI '18)*. ACM, New York, NY, USA, Article 515, 13 pages. https://doi.org/10.1145/3173574.3174089

[42] Huizhong Ye, Chi-Jung Lee, Te-Yen Wu, Xing-Dong Yang, Bing-Yu Chen, and Rong-Hao Liang. 2022. Body-Centric NFC: Body-Centric Interaction with NFC Devices Through Near-Field Enabled Clothing. In *Designing Interactive Systems Conference* (Virtual Event, Australia) *(DIS '22)*. Association for Computing Machinery, New York, NY, USA, 1626–1639. https://doi.org/10.1145/3532106.3534569

[43] Hui-Shyong Yeo, Ryosuke Minami, Kirill Rodriguez, George Shaker, and Aaron Quigley. 2018. Exploring Tangible Interactions with Radar Sensing. *Proc. ACM Interact. Mob. Wearable Ubiquitous Technol.* 2, 4, Article 200 (dec 2018), 25 pages. https://doi.org/10.1145/3287078

[44] Oren Zuckerman, Saeed Arida, and Mitchel Resnick. 2005. Extending Tangible Interfaces for Education: Digital Montessori-Inspired Manipulatives. *CHI 2005: Technology, Safety, Community: Conference Proceedings - Conference on Human Factors in Computing Systems*. https://doi.org/10.1145/1054972.1055093